



Azadirachta indica Seed Oil Epoxidation Using Sulfuric Acid as a Catalyst; Response Surface Methodology and Particle Swarm-Based Evaluation and Optimization

Kenechi Nwosu-Obieogu¹ · Emmanuel Oke¹ · Oladayo Adeyi¹ · Goziya Williams Dzarma¹ · Aguele Felix¹ · Chiemenem Linus¹ · Akatobi Noble¹ · Kalu Chinweike¹ · Christian Goodnews¹

Received: 28 September 2023 / Accepted: 30 July 2024
© Indian National Academy of Engineering 2024

Abstract

Response surface methodology (RSM) was employed in this study to optimize the epoxidation of *Azadirachta indica* seed oil (AISO) in the presence of sulfuric acid as a catalyst. The independent variables were (catalyst concentration, time, and temperature) while iodine and oxirane values were the dependent variables. The (analysis of variance) ANOVA showed a second-order polynomial model with a predicted R^2 value of 0.8530 for iodine value and 0.8114 for oxirane value indicating the model's acceptability. The experimental results [one factor at a time (OFAT), 3D, and contour plots] showed that the process parameters (catalyst concentration, time, and temperature) had a significant impact on the iodine and oxirane value. The model established from ANOVA was optimized using a metaheuristic algorithm—Particle Swarm Optimization (PSO) and validated with RSM-predicted optimal values. The optimal (RSM) iodine value (12.7 g $I_2/100g$) and oxirane value of 4.910% were obtained at a catalyst concentration of 1.2 mol/L, a reaction time of 14,400 s, and a reaction temperature of 50 °C with a desirability of 1.000. PSO optimal iodine value (7.9 g $I_2/100g$) and oxirane value of 5.172% were obtained at the same optimal conditions. The results demonstrated that PSO was slightly better than RSM. Nevertheless, both results optimized AISO efficiently and agreed with the experimental data (iodine value—8.25 g $I_2/100g$; oxirane value—5.134%). The characterizations result via FT-IR (Fourier transform infrared spectroscopy) and GCMS (gas chromatography mass spectrometer) indicated the successful formation of epoxides on AISO for its utilization as intermediates for lubricants and polyols. These results showed that the proposed models enhanced the stability of the AISO epoxidation and reduced the cost and processing time.

Keywords *Azadirachta indica* seed oil · Epoxidation · Response surface methodology · Particle swarm optimization · Catalyst

Introduction

The demand for biopolymeric resins of natural origin with practical applications must be emphasized due to issues associated with a petroleum-based resin, such as non-degradability and renewability of the product, fluctuation of oil price, and environmental pollution. This has instigated researchers to search for renewable materials for sustainable

epoxide development (Okieimen et al. 2002; Nwosu-obieogu et al. 2020).

Vegetable oils have been considered an excellent alternative source for the production of epoxides; hence, *Azadirachta indica*, *huracrepitan*, and rapeseed oil are some of the vegetable oils considered for this process due to their inedibility and non-competitiveness with food crops (Any et al. 2016; Aguele et al. 2021; Milchert et al. 2010).

Azadirachta indica tree belongs to tropical Southeast Asia and the family *Meliaceae* (Nwosu-obieogu et al. 2022a). It multiplies in tropical and semi-tropic climates and can reach a height of 35–40 m (115–131 ft.), surviving in arid conditions. AISO is a vegetable oil pressed from seeds of the *Azadirachta indica* fruits. The oil yield differs widely in the literature from 25 to 45%, as reported by Yash Roy and

✉ Kenechi Nwosu-Obieogu
kenenwosuobie@mouau.edu.ng

¹ Chemical Engineering Department, Michael Okpara University of Agriculture, Umudike, Nigeria

Gupta (2000) and Adepoju and Olawale (2015), respectively; this compares favourably with *luffa* oil yield of 27.7%, as reported by Nwosu-Obieogu and Umunna (2021) on *luffa* oil extraction modeling and optimization.

Reports have shown that *Azadirachta indica* oil contains triglycerides that can be epoxidized (Kareemullah et al. 2021; Sahu and Mohanty 2017). These epoxides can be utilized as resins for plastics and paint production and as raw materials to prepare chemical compounds, such as alcohols, glycols, and olefinic and carbonyl compounds (Dinda et al. 2016). Kareemullah et al. (2021) developed and analyzed epoxidized *Azadirachta indica* oil-based lubricants. Sahu and Mohanty (2017) studied the epoxidation of oleic-rich *Azadirachta indica* oil over a bio-waste catalyst.

Epoxidation reaction converts the double bonds of fatty acid triglycerides in oil to oxirane groups. (Turco et al. 2019; Nwosu-obieogu et al. 2022a). Specifically, the unsaturated fatty acids' carbon-carbon double bonds (C=C) react with a peracid to form epoxide groups (oxirane rings). According to studies, process variables such as temperature, time, and catalyst concentration influence oil epoxidation (Nwosu et al. 2021). According to Matusiak and Milchert (2018), as the reaction temperature rises, the time required to achieve high efficiency decreases; however, a high temperature intensifies side reactions during epoxide formation. The type of oxidizing agent (Dinda et al. 2016), the molar ratio of reactants (Matusiak and Milchert 2018), and the intensity of mixing (Goud et al. 2006) are all factors that influence the epoxidation reaction. As a result, modeling and optimization of process variables will aid in enhancing the process reaction, developing the optimal yield, and establishing the relationship between the process parameters (temperature, time, and catalyst concentration) and the oxirane value (Nwosu-obieogu and Umunna 2021). An optimal oxirane value of 3.96348% for melon seed oil and 4.07169% for huracerepitan seed oil reported by Nwosu-obieogu et al. (2024) and Aguele et al. (2021) respectively confirm that vegetable seed oil can be suitably epoxidized applying same epoxidation procedure.

RSM is a statistical technique applied in the design and analysis of experimental data. It also models and optimizes chemical processes and products, improving existing product designs (Onoji et al. 2017). The RSM model helps predict our independent variables' desired response (Oke et al. 2021). Compared to the linear regression technique, RSM develops the desired optimal solution at a reduced time (Nwosu-obieogu et al. 2022b). Various studies have been carried out using RSM to optimize epoxide yield from vegetable seed oil such as *Hevea brassiliensis* seed

oil (Nwosu-obieogu et al. 2020), sandbox seed oil (Aguale et al. 2021).

Metaheuristic soft-computing techniques such as particle swarm optimization (PSO), genetic algorithm (GA), and Grey wolf optimizer (GWO) have been a subject of focus in modeling complex chemical variables (Oke et al. 2020; Nwosu-obieogu et al. 2022c). These models apply a sensitivity approach to measure the parametric impact on the outputs or performance of the process (Nwosu-obieogu et al. 2022d). Among these techniques, PSO stands out in chemical process modeling and optimization.

PSO is inspired by animal collective behavior; the set of candidate optimization problem solutions is defined as particles' swarms flowing through space and specifying trajectories (Khayati 2020; Nassef et al. 2019). These paths are determined by their best performances and those of their neighbors. This algorithm is a robust and stochastic soft computing technique for locating the global optimum in a large search space. It is a simple, more effective technique that converges faster than other metaheuristic techniques while requiring less time (Jalil et al. 2022). Researchers have studied the utilization of PSO in predicting chemical processes. Nassef et al. (2019) compared fuzzy modeling with PSO in biodiesel production enhancement from microalgae. Kadi et al. (2019) optimized the transesterification kinetics of biodiesel production from rapeseed oil using PSO, Fang et al. (2022) predicted industrial propane dehydrogenation process using PSO, and Khayati (2020) predicted silver nanoparticles green synthesis using PSO. Their observations indicated the efficiency of PSO in modeling and optimizing chemical processes. Also, few studies have been carried out using PSO to optimize the epoxidation process, such as the optimization of styrene epoxidation by Huang et al. (2019). Development of hydrolyzed dihydroxy stearic acid (DHSA) from epoxidized oleic acid (EOA) by Jalil et al. (2022). Formation of dihydroxystearic Acid (DHSA) from epoxidized palm oleic acid by Jalil et al. (2020). Some researchers reported on the combination of RSM and PSO in process optimization, the total colour difference of pineapple fortified rasgulla processing (Sarkar et al. 2020), the optimization of the FDM process for flexural strength (Saad et al. 2021), the parametric optimization in making of Nimoic-263 alloy (Rao and Venkaiah 2015), the valorization of *Citrus unshiu* biowastes to value-added products (Poyraz et al. 2021) and methylene blue removal using silver nanoparticles from water (Khajeh et al. 2013). However, no documented information exists about AISO epoxidation optimization using RSM and PSO. Therefore, this study aims to model and optimize the process conditions of oil epoxidation from *Azadirachta indica* seeds using PSO and RSM.

Materials and Methods

Material and Equipment

AISO, aqueous hydrogen peroxide 30%, acetic acid 98%, sulfuric acid 98%, hexane 99%, and ethanol were purchased at technical grade from Vinod Chemicals Aba, Abia State, Nigeria. Also, a three-necked round bottom flask (250 mL capacity), magnetic heater, thermometer, reflux condenser, and funnel were obtained from Conraws Ltd. Enugu, Nigeria.

Methodology for AISO Epoxidation

30 g of AISO was placed in the beaker, and 4 g of acetic acid was added to the three-necked round bottom flask; after 5 min, 0.75% w/w of sulfuric acid was added, the mixture was stirred continuously for 30 min. Then, 16.15 g of 30 wt% aqueous hydrogen peroxide was added dropwise to the reaction mixture; the mole ratio of the component used is 1:1.5:0.5, representing the oil, hydrogen peroxide, and acetic acid. After the complete addition of hydrogen peroxide, the mixture was heated under reflux at the temperature (65 °C) and with rapid stirring to achieve fine oil dispersion. 10 g of Na₂CO₃ was first dissolved in 100 mL of distilled water, and the collected samples of Epoxidised (AISO) were dissolved in distilled water to remove the free acids and other unreacted components. A separating funnel separated it (Nwosu-obieogu et al. 2024).

Modeling and Optimization of Epoxidation of *Azadirachta indica* Seed Oil Using Response Surface Methodology

The experiment was designed using Design-Expert version 10, utilizing the box-behnken technique on three factors and a three-level. The independent variables are the catalyst concentration, time, and temperature; the iodine and oxirane values were considered the response. Seventeen experimental runs were generated from the simulation (Nwosu-obieogu et al. 2020; Oke et al. 2021). Design expert employed a one-way ANOVA to assess the responses independently. Also, the p-value should be less than 0.05 for the model to be significant. The experimental design is presented in Table 1.

Modeling and Optimizing *Azadirachta indica* Seed Oil Epoxidation Using Particle Swarm Optimization

PSO is a stochastic optimization approach miming birds' dynamic movements and communication. The technique utilizes theoretical models comprising a swarm searching for

Table 1 Summary of the experimental factors coding

Factor	Name	Units	Level		
			-1	0	1
A	Concentration of the catalyst	mol/L	0.6	1.2	1.8
B	Time	s	14,400	21,600	28,800
C	temperature	°C	50	60	70

Table 2 The PSO parameters

Iteration	10
Population	17
C ₁	2
C ₂	2
Wmax	0.9
Wmin	0.4

space to explore the location for the best solution to attain the global optimum solution (Fang et al. 2022; Jalil et al. 2022; Khayati 2020). The particle's position update rule is shown in Eqs. (1) and (2)

$$p(k+1) = p(k) + v(k+1) \quad (1)$$

$$v(k+1) = wv(k) + c_1r_1(pBest - p) + c_2r_2(gBest - p) \quad (2)$$

where p is the particle's current position; v is the particle's velocity; c₁ and c₂ are the cognitive and social acceleration constants; pbest and gbest are the particles and global best position of the swarm, respectively; r₁ and r₂ are two random numbers, between 0 and 1; empirical results have shown that a constant inertia wmax = 0.9, wmin = 0.4, acceleration coefficient c₁ = 2, c₂ = 2 and iteration of 10 provides good convergence in the resolution and optimization of systems proven in the literature and our systems (Nassef et al. 2019; Huang et al. 2019; Jalil et al. 2020). The PSO program was executed in MATLAB 8.4 (R2015b) software environment, and the parameters used in this work are illustrated in Table 2.

Characterization of the Pure and Epoxidized AISO

Standard procedures described by the Association of Official Analytical Chemists (AOAC 2003) were used to characterize the pure and epoxidized AISO.

Iodine Value

Wijs solution was employed to determine the iodine value of the pure and epoxidized AISO. The solution consists of iodine monochloride (ICI) in glacial acetic acid and carbon

tetrachloride. The unsaturated bonds present take up the iodine to saturate the double bonds, and the remaining unabsorbed iodine is then titrated using sodium thiosulphate (Nwosu-obieogu et al. 2024).

The iodine value (IV) was calculated from Eq. (3) below.

$$IV = \frac{(B - S) \times M \times 12.69}{W} \quad (3)$$

where:

IV = iodine value of samples, S = volume of Na₂S₂O₃ used for sample (mL), B = volume of Na₂S₂O₃ used for blank (mL), W = weight of sample used (g), M = molarity of the Na₂S₂O₃ used.

Oxirane Value

The oxirane value was analyzed by the direct method of HBr in AA (Paquot), as presented in Standard Methods for the Analysis of Oils compiled by the Union of Pure and Applied Chemistry (Nwosu-obieogu et al. 2024).

The oxirane value of the AISO was evaluated using the formula in Eq. (4):

$$OV = \frac{(B - S) \times M \times A_o \times 100}{1000W} \quad (4)$$

where:

A_o = atomic weight of oxygen
 M = molarity of the NaOH used
 W = weight of sample used (g)
 S = volume of NaOH used for sample (mL)
 B = volume of NaOH used for blank (mL)

Specific Gravity

The specific gravity was obtained using Eq. (5) below, adopted by Nwosu-obieogu et al. (2024).

$$\text{Specific gravity} = \frac{\text{weight of oil}}{\text{weight of the equal volume of water}} \quad (5)$$

Fourier Transform Infrared Spectroscopy (FT-IR)

FTIR analytical techniques were complementary methods (after chemical processes) to characterize structural functionalities in the pure and epoxidized AISO (Nwosu-obieogu et al. 2024). FTIR spectrum of the epoxidized oil was recorded with a Shimadzu 8400SFTIR spectrophotometer

over the range 4500 – 350 cm⁻¹ using ten scans at a resolution of 4 cm⁻¹.

Gas Chromatography–Mass Spectrometry (GC–MS)

The GCMS of the pure and epoxidized AISO was prepared by dissolving 50 mg of the sample in 10 mL of toluene, 0.2 mL of Tetramethylammonium hydroxide (TMAH), and 4 mL of water placed in a conical flask, the mixture was allowed to settle at a temperature of 80 °C and a flow rate of 1.5 mL/min. The fatty acid profiles of the samples were analyzed. The peaks were identified on a mass-selective detector interfaced with a GCMS (Nwosu-obieogu et al. 2022c).

Results and Discussion

Physicochemical Properties of Pure and Epoxy AISO

The physicochemical properties of AISO are shown in Table 3; the iodine value of 86.73 indicates that the oil is a non-drying oil consisting predominantly of unsaturated fatty acids; it decreased when the oil was epoxidized, which confirms a successful transformation of the unsaturated triglycerides to oxirane rings and reduction in structural residues when epoxidized, the oxirane value of 5.134 indicates the level of oxirane oxygen content available after successful epoxide formation, the specific gravity increased due to the decrease in unsaturation of the AISO. These findings agree with reports of rubber seed oil and huracreptan seed oil epoxidation by Nwosu-obieogu et al. (2020) and Aguele et al. (2021), respectively.

One Factor at a Time Analysis for Epoxidation of *Azadirachta indica* Seed Oil

Table 4 shows the effect of the concentration of the catalyst, time, and temperature on the iodine and oxirane value of the EAISO. The result showed that at a concentration of 1.8, the maximum oxirane value for the catalyst was obtained. As the catalyst concentration increased, the oxirane value increased from 1.56 to 2.10. It then decreased at a catalyst concentration of 2.4; the decrease is due to cleavage on the oxirane ring while time and temperature were kept constant at 21,600 s and 60 °C, respectively, at a reaction time of 14,400 s, constant

Table 3 Physicochemical properties of pure and epoxy AISO

Properties	AISO	EAISO
Iodine value (gI ₂ /100g)	86.73	15.00
Oxirane value (%)	–	5.134
Specific gravity	0.923	0.970

Table 4 One factor at a time (OFAT) parameter effect on oxirane value

S/N	Catalyst conc (mol/L); time—21,600 s, temperature—60 °C	Iodine value (gI ₂ /100g)	Oxirane value (%)	Time (s); catalyst conc.—1.8 mol/L, temperature—60 °C	Iodine value (gI ₂ /100g)	Oxirane value (%)	Temperature (°C); time—21,600 s, catalyst conc.—1.8 mol/L	Iodine value (gI ₂ /100g)	Oxirane value (%)
1	0.6	36.72	1.82	14,400	18.9	4.62	50	19.88	3.83
2	1.2	31.01	1.93	18,000	21.7	2.23	55	42.36	1.49
3	1.8	25.4	2.10	21,600	25.02	2.17	60	38.2	1.75
4	2.4	41.2	1.56	25,200	29.43	1.98	65	21.7	2.23
5	3.0	31.01	1.93	28,800	20.76	2.81	70	24.2	2.38

catalyst concentration (1.8 mol/L) and temperature (60 °C), the maximum oxirane value (4.62) was obtained, hence progressively reduced with increase in time, at a temperature of 50 °C, the highest oxirane value (3.83) was obtained. In comparison, temperature and catalyst concentration were kept constant at 21,600 s and 1.8 mol/L; furthermore, an increase in temperature decreased the oxirane value. The observation may be attributed to the reversible reaction of the peroxyacetic acid formed in situ and the undesired reactions of the ring-opening of the oxirane group. Also, it was observed that as the iodine value decreased, the oxirane value increased, indicating the disappearance of the C=C bonds on the AISO for the attachment of an oxirane ring; these findings indicate that process parameters (catalyst concentration, time, and temperature) had a significant effect on the oxirane value, with the impact of time and temperature more economically feasible. The design of the experiment was developed from the process parameters. This result coincides with the studies of Okieimen et al. (2002) for rubber seed oil, (Matusiak and Milchert 2018) for canola oil, and Nwosu-obieogu et al. (2022a) on the epoxidation of *Azadirachta indica* oil using microwave sulfonated melon seed peel catalyst.

Modeling of Epoxidation of *Azadirachta indica* Seed Oil Using Response Surface Methodology

The experimental design for the epoxidation of the AISO was analyzed using the Box Behnken design, which implemented the RSM technique in Design Expert 10.0. The experimental values of the dependent variable (iodine and oxirane value) with their corresponding independent parameters are presented in Table 5. The minimum iodine value (8.32 g I₂/100g) and the maximum oxirane value (5.134%) were obtained at the concentration of the catalyst (1.2), time (14,400 s), and temperature (50 °C); the results obtained showed the effect of varying the process variables on the epoxide formation (Aguete et al. 2021; Nwosu-obieogu et al. 2024; Nwosu-obieogu and Umunna 2021).

The multiple regression analysis of the data gave a second-order polynomial equation in coded factors shown in Eqs. (6) and (7)

Table 5 Experimental run for the EAISO development

Run	Catalyst dosage (mol)	Time (s)	Temperature (°C)	Iodine value (gI ₂ /100g)	Oxirane value (%)
1	1.8	21,600	70	23.42	3.2
2	1.8	21,600	50	20.21	4.64
3	1.2	21,600	60	26.19	3.4
4	0.6	14,400	60	17.32	4.75
5	1.2	21,600	60	26.19	3.4
6	0.6	28,800	60	31.01	2.43
7	1.2	21,600	60	26.19	3.4
8	1.2	14,400	50	8.25	5.134
9	0.6	21,600	50	43.08	1.75
10	1.2	21,600	60	26.19	3.4
11	1.8	28,800	60	34.75	2.4
12	1.2	14,400	70	22.05	4.16
13	1.2	21,600	60	26.19	3.4
14	0.6	21,600	70	27.3	3.56
15	1.2	28,800	70	26.2	2.21
16	1.2	28,800	50	30.01	2.58
17	1.8	14,400	60	19.89	5.09

$$\begin{aligned} \text{Iodine value (gI}_2\text{/100g)} = & +26.19 - 5.87A \\ & - 0.1825B - 3.63C - 6.33AB + 4.75AC \\ & + 2.22BC - 3.41A^2 - 3.66B^2 + 5.72C^2 \end{aligned} \quad (6)$$

$$\begin{aligned} \text{Oxirane value (\%)} = & +3.40 + 0.6968A - 0.5057B \\ & + 0.2200C + 0.5910AB - 0.8125AC - 0.5325BC \\ & + 0.7005A^2 + 0.2505B^2 - 0.8130C^2 \end{aligned} \quad (7)$$

where A is the concentration of the catalyst(mol/L), B—time(s) and C—temperature (°C).

The plot of the predicted vs. the actual response of the iodine and oxirane value of AISO was observed in Figs. 1a and 2a; the figure shows that the predicted values are quite close to the experimental values, which validates the reliability of the model and shows a good fit. The

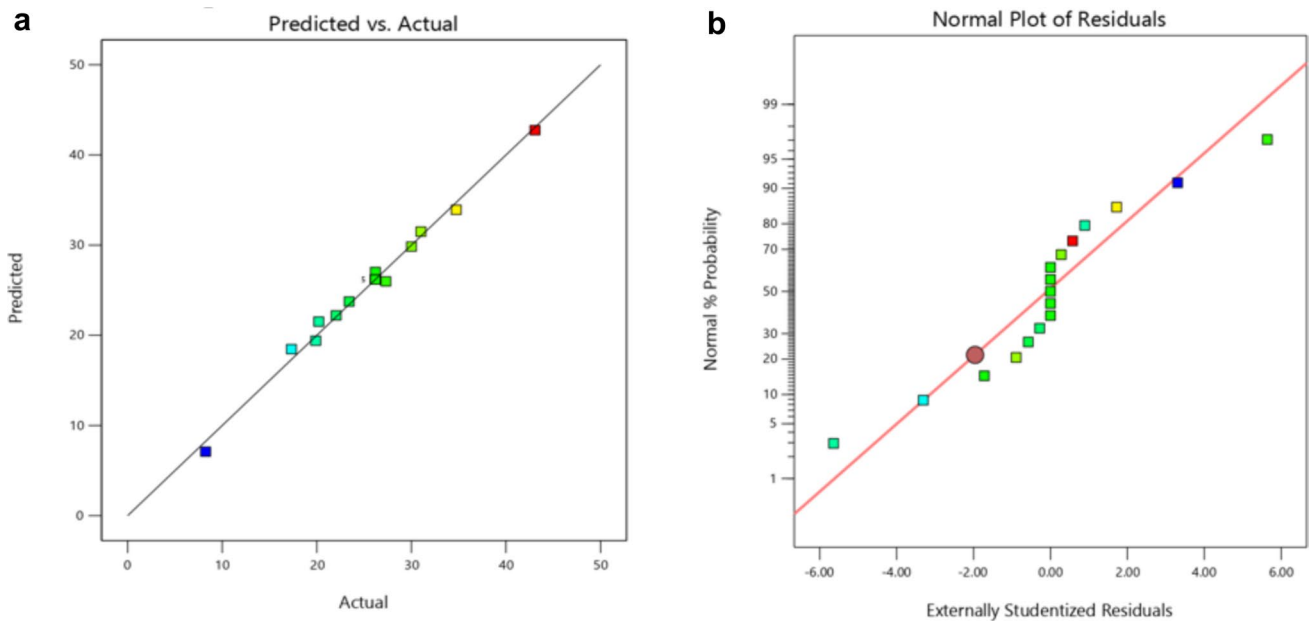


Fig. 1 a Predicted against actual plot for iodine value. b Normal plot of residuals for iodine value

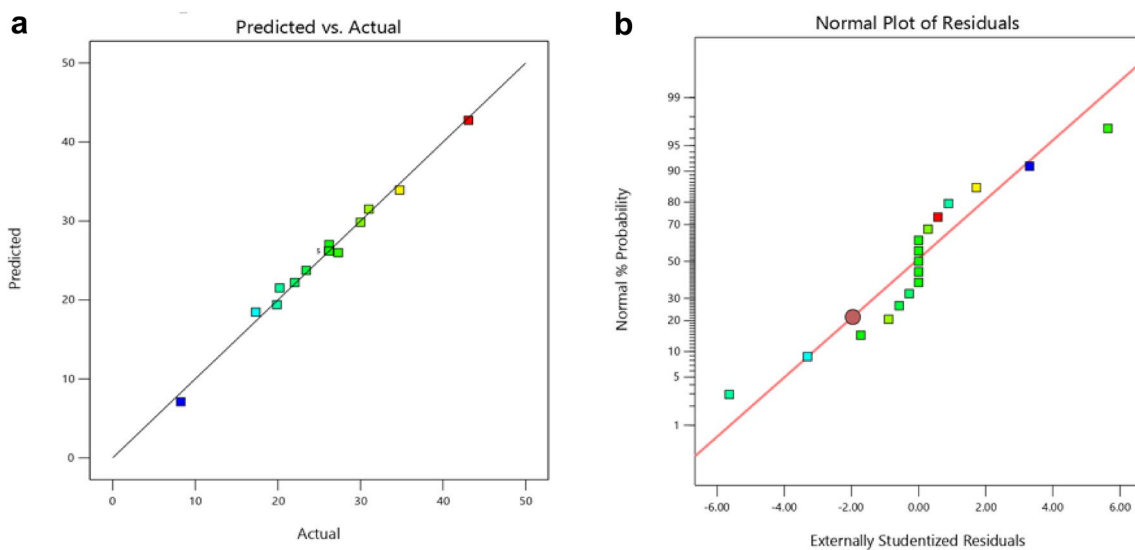


Fig. 2 a Predicted against actual plot for oxirane value. b Normal plot of residuals for oxirane value

points were distributed around a straight line, indicating the model's high level of predictability. Figures 1b and 2b show the relationship between the model predictions and actual experimental results for the iodine and the oxirane value; the diagonal can be a line of perfect prediction; points above the line represent model under-prediction, while the points below represent model over-prediction. It helped ascertain if the models were satisfactory. The data

was plotted against a theoretical normal distribution. The projections formed an approximately straight line, and a departure from this line indicates a falling out from a normal distribution. A closer observation of this plot shows that most points are closer to the line, showing that the values were normally distributed (Aguele et al. 2021; Matysiak and Milchert 2018; Nwosu-obiogou et al. 2022d).

Table 6 ANOVA result of AISO iodine value

Source	Sum of squares	df	Mean square	F-value	p-value	
Model	883.35	9	98.15	83.88	<0.0001	Significant
A-catalyst dosage	275.42	1	275.42	235.38	<0.0001	Significant
B-time	0.2664	1	0.2664	0.2277	0.6478	Not significant
C-temperature	105.71	1	105.71	90.34	<0.0001	Significant
AB	160.40	1	160.40	137.08	<0.0001	Significant
AC	90.16	1	90.16	77.05	<0.0001	Significant
BC	19.76	1	19.76	16.89	0.0045	Significant
A ²	49.00	1	49.00	41.87	0.0003	Significant
B ²	56.44	1	56.44	48.24	0.0002	Significant
C ²	137.94	1	137.94	117.89	<0.0001	Significant
Residual	8.19	7	1.17			
Lack of fit	8.19	3	2.73			
Pure error	0.0000	4	0.0000			
Cor total	891.54	16				
Std. dev.	1.08	R ²	0.9908			
Mean	25.56	Adjusted R ²	0.9790			
C.V. %	4.23	Predicted R ²	0.8530			
		Adeq precision	42.9733			

ANOVA Analysis of Epoxidation of *Azadirachta indica* Seed Oil

ANOVA statistically evaluated each model's significance and their interactions; in Table 6, the iodine value result displayed the high impact of all the terms of the model except for the single term (B), based on the f-value and p-values, the linear terms (A and C), interaction terms, and quadratic terms impacted iodine value significantly. Similar results

were reported by Nwosu-obiogou et al. (2020), Aguele et al. (2021), and Matusiak and Milchert (2018) on the epoxidation of rubber, *huracrepitan*, and canola seed oil, respectively. The standard deviation (1.08), mean (25.5, C.V.% (4.23), f-value (65.19), p-value (0.0001), and adequate precision (42.9733) indicate that the model is acceptable and strong for optimization. The lack of fit of the model (8.19), which is not significant, supports a good fit for the model. The models' fitness was expressed by the coefficient

Table 7 ANOVA result of AISO oxirane value

Source	Sum of squares	df	Mean Square	F-value	p-value	
Model	16.35	9	1.82	65.19	<0.0001	Significant
A-catalyst dosage	3.88	1	3.88	139.36	<0.0001	Significant
B-time	2.05	1	2.05	73.43	<0.0001	Significant
C-temperature	0.3872	1	0.3872	13.89	0.0074	Significant
AB	1.40	1	1.40	50.13	0.0002	Significant
AC	2.64	1	2.64	94.75	<0.0001	Significant
BC	1.13	1	1.13	40.70	0.0004	Significant
A ²	2.07	1	2.07	74.14	<0.0001	Significant
B ²	0.2642	1	0.2642	9.48	0.0178	Significant
C ²	2.78	1	2.78	99.86	<0.0001	Significant
Residual	0.1951	7	0.0279			
Lack of fit	0.1951	3	0.0650			
Pure error	0.0000	4	0.0000			
Cor total	16.55	16				
Std. dev	0.1669	R ²	0.9882			
Mean	3.46	Adjusted R ²	0.9731			
C.V. %	4.82	Predicted R ²	0.8114			
		adeq Precision	27.9199			

of determination of R^2 (0.9908), adjusted R^2 (0.9790), and predicted R^2 (0.8530), suggesting consistency and a good agreement between the experimental and the predicted data. Table 7 presents the findings of the variance analysis for oxirane value. The model's R^2 , adjusted R^2 , and predicted R^2 were 0.9882, 0.9731, and 0.8114, respectively. These values indicate a strong fit for the model and a high correlation between the observed and expected values. The whole model demonstrated statistical significance (p -value < 0.05). The single, interaction, and quadratic factors were found to be significant. The standard deviation (0.1669), coefficient of variation (C.V %) (4.82), and adequate precision (27.9199) suggest that the model is acceptable and resilient for optimizing oxirane value, these results corroborate with the

findings of Nwosu-obieogu et al. (2024) on melon seed oil epoxidation.

Parametric Studies of Epoxidation of *Azadirachta indica* Seed Oil

The effect of the interaction terms of the process parameter on the iodine value is shown in Fig. 3; it was observed that an increase in catalyst concentration and time led to a reduction in the iodine value; also, in Fig. 3b, an increase in catalyst concentration and temperature led to a decline in the iodine value, in fig c, an increase in time and temperature led to a decrease in the iodine value, this observation can be attributed to C=C bonds present in the oil that is been

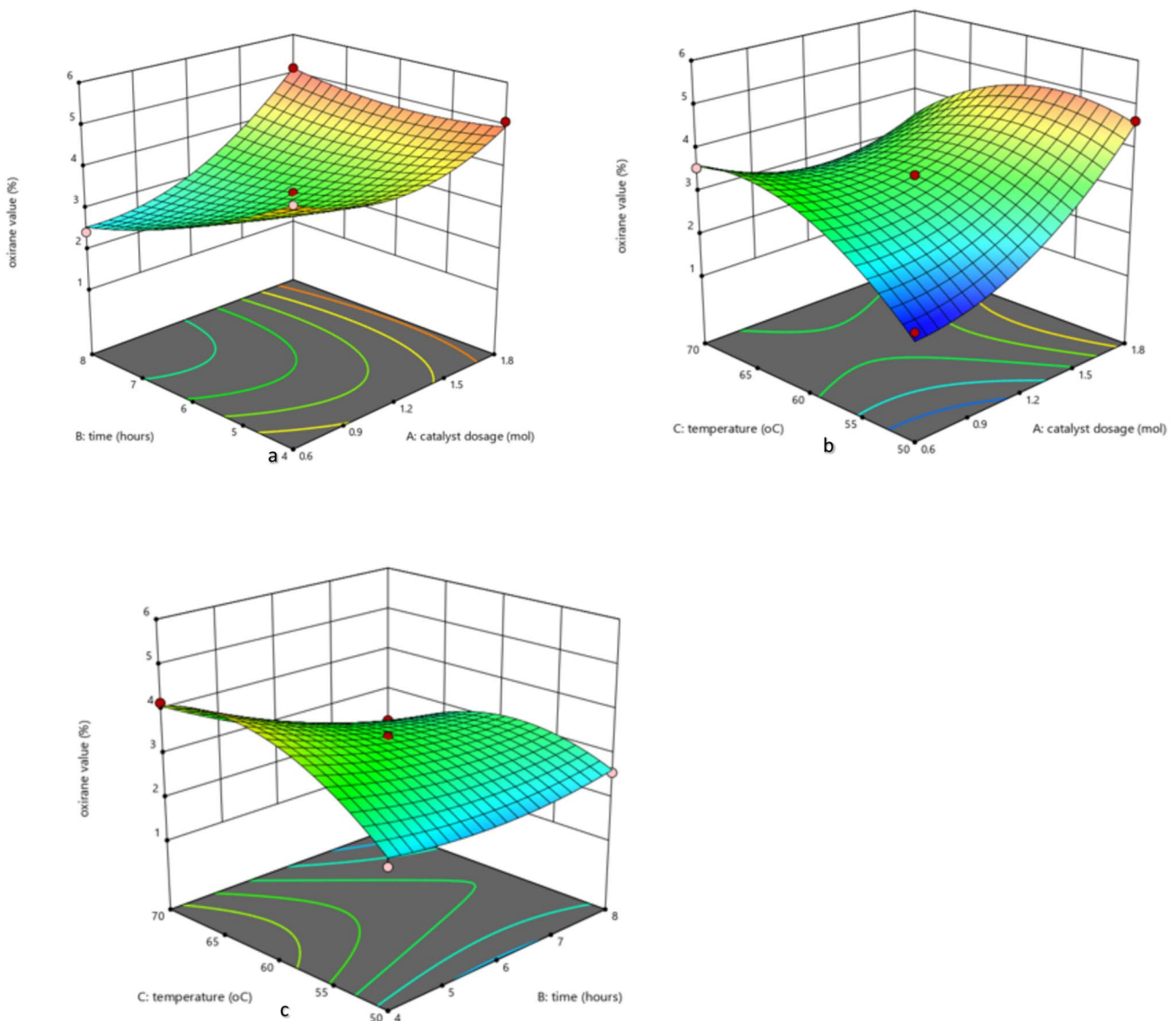


Fig. 3 a Effect of catalyst concentration and time (temperature—60 °C). b Catalyst concentration and temperature (time—21,600 s). c Effect of time and temperature (catalyst concentration—1.2 mol/L) on the iodine value

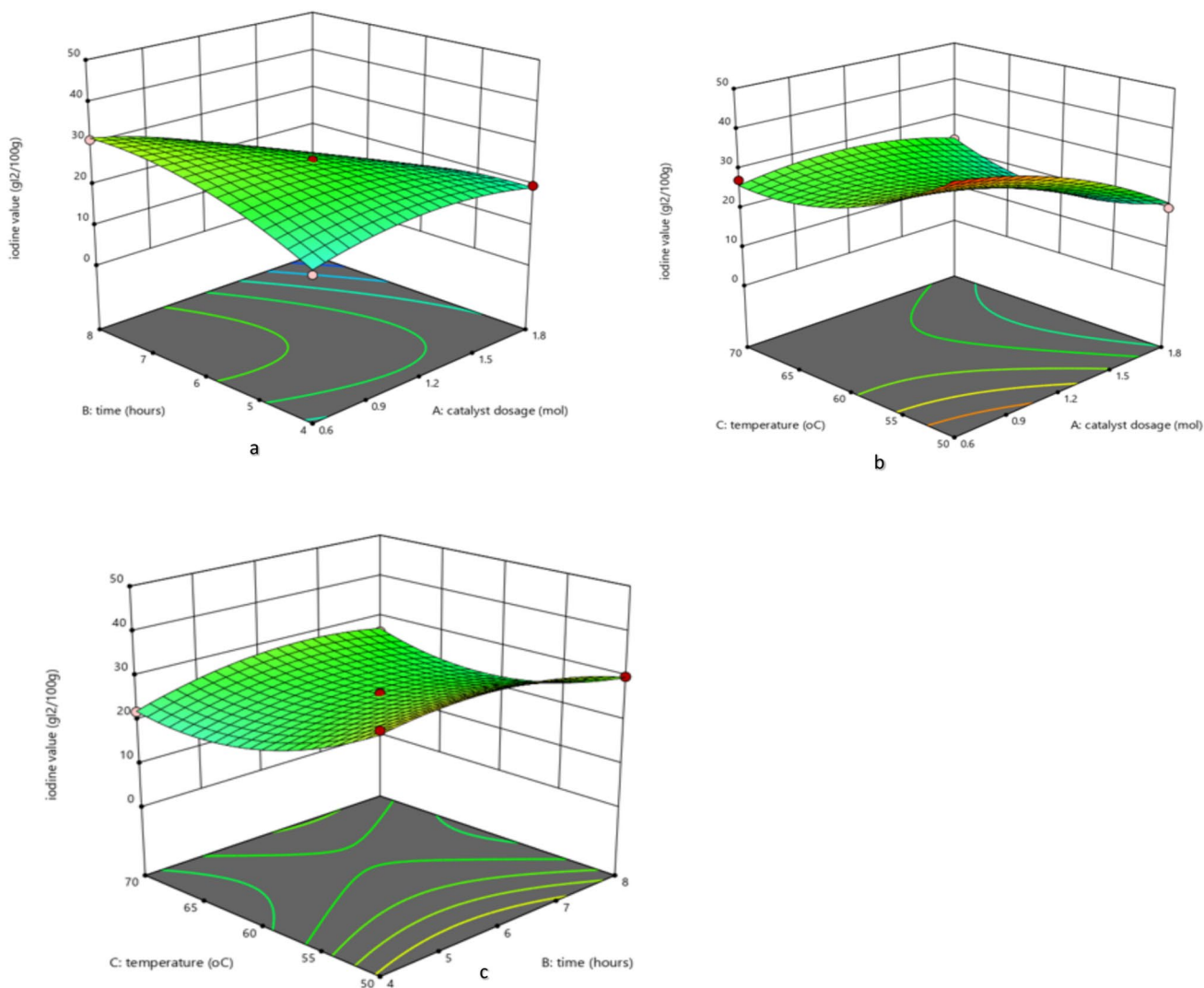


Fig. 4 **a** Effect of catalyst concentration and time (temperature—60 °C). **b** Catalyst concentration and temperature (time—21,600 s). **c** Effect of time and temperature (catalyst concentration—1.2 mol/L) on the oxirane value

converted to epoxides, also this results to the more active site with lesser reacting species (Jalil et al. 2022). The effect of the concentration of the catalyst and time on the oxirane value is presented in Fig. 4. The result showed that a rise in the concentration of the catalyst increases the oxirane value; this is attributed to the sufficient catalyst that proceeded the reaction faster; subsequently, a rise in the reaction time increased the oxirane value, depicting the unsaturated fatty acid triglyceride conversion to oxirane (Nwosu-obieogu et al. 2024). Figure 4 also shows the combined effects of the catalyst concentration and temperature on the oxirane value. The 3D plot showed that an increased catalyst concentration increases the oxirane value.

Similarly, an increase in the reaction temperature increases the oxirane value. The combined effects of reaction time and temperature on the oxirane value, as shown in Fig. 4, depicted that an increase in the reaction time increases the oxirane value, confirming that epoxides are formed at higher temperatures (Oke et al. 2021). In contrast, the reaction's temperature decreases the oxirane value; this observation is attributed to the reversible reaction of the peracetic acid formation. The observations show that the process parameters significantly impacted the oxirane value, and the quadratic effects had more impact on the oxirane value than the interaction terms with negative effects. This corroborates the findings of Nwosu-obieogu et al. (2020) on rubber seed oil epoxidation and Aguele et al. (2021) on huracrepitana seed oil epoxidation.

Table 8 Comparison of the optimal values of EAISO by RSM and PSO techniques

Methods	Catalyst concentration (mol/L)	Time(s)	Temperature (°C)	Iodine value (gI ₂ /100g)	Oxirane value (%)
Experimental	1.2	14,400	50	8.25	5.134
RSM	1.2	14,400	50	12.7	4.910
PSO	1.2	14,400	50	7.9	5.172

Optimization of the Epoxidation of *Azadirachta indica* Seed Oil Using Response Surface Methodology and Particle Swarm Optimization

AISO epoxidation optimization using the RSM and PSO optimization tools is shown in Table 8. At a concentration of catalyst of 1.200 mol/L, 14,400 s reaction time, and temperature of 50 °C, the optimal iodine value—RSM(12.7), experimental (8.25) and PSO (7.9) gI₂/100g and oxirane value—RSM, (4.910%), experimental (5.134%) and PSO of 5.172% were obtained. For the performance metrics, both techniques (RSM and PSO) suggested a good agreement with the experimental value at minimal residual error, as the goal of the process was actualized with a reduced iodine value and a high oxirane value even though PSO gave the best optimal condition; the findings also show the efficiency of PSO in optimizing the epoxidation process of AISO. This result conforms with the reports of Matusiak and Milchert (2018) on the optimization of the canola oil epoxidation process and Oke et al. (2021) on the rubber seed oil epoxidation using a hybrid genetic algorithm.

Characterization of the Epoxidized AISO

Fourier Transform Infrared Spectroscopy (FTIR)

The FTIR graph for the pure AISO shown in Fig. 5 showed peaks of 2922.2 and 2723.1 cm⁻¹, indicating (=C–H) stretch alkanes. The peak (1744.4 cm⁻¹) validates the presence of carbon–carbon double bonds (C=C) in the pure AISO; this indicates that the oil contains unsaturated fatty triglycerides that can be suitably epoxidized. (Yigezu 2021; Jalil et al. 2022). 1461.1 cm⁻¹ corresponds to the C–C ethylene stretch, indicating that the oil can be used for the epoxidation process; 1159.2 cm⁻¹ stated the presence of C–H. Double bond groups suggest the oil has not been activated or used for any reaction. The FTIR spectra of the H₂SO₄ epoxy *Azadirachta indica* oil in Fig. 6 showed the presence of O–H stretching alcohol at 3381.9 peaks indicating that the epoxidation process, as well as the utilization of sulfuric acid, the (C=C) bond disappears, there is an absorption band of 1714.6 cm⁻¹ in the EAISO spectrum which showed the presence of cyclic ether group of the epoxy functionality. This analysis agrees with the

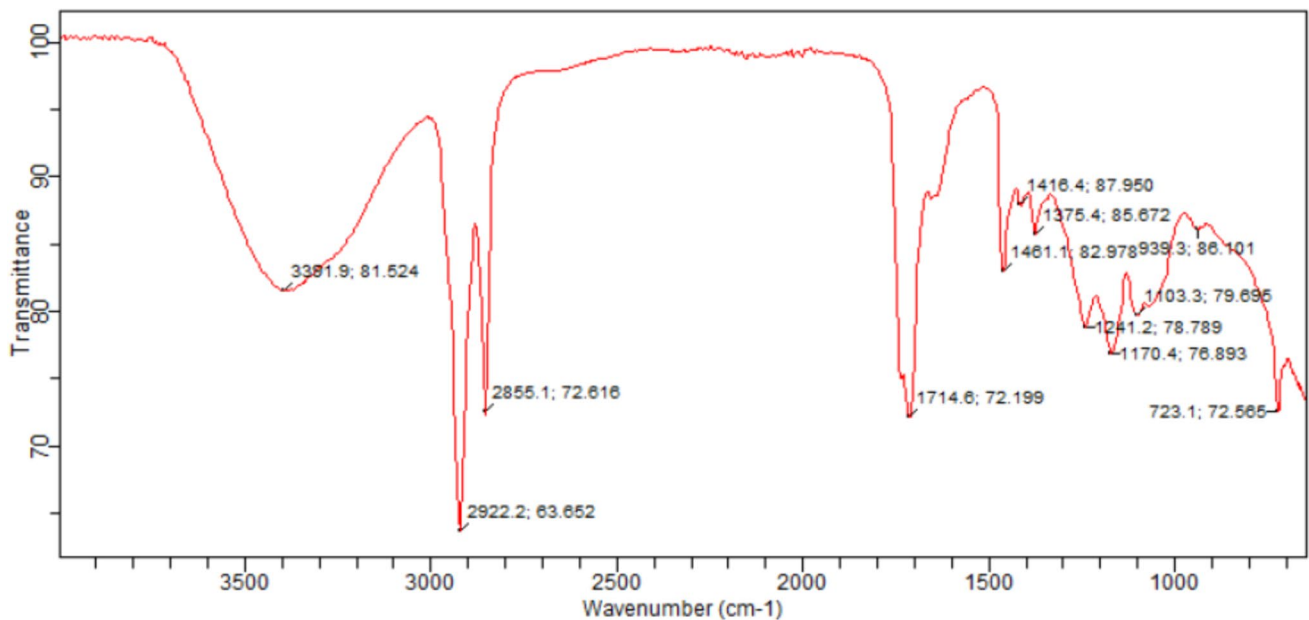


Fig. 5 FTIR for pure *Azadirachta indica* oil

Fig. 6 FTIR for H₂SO₄ epoxy *Azadirachta indica* oil

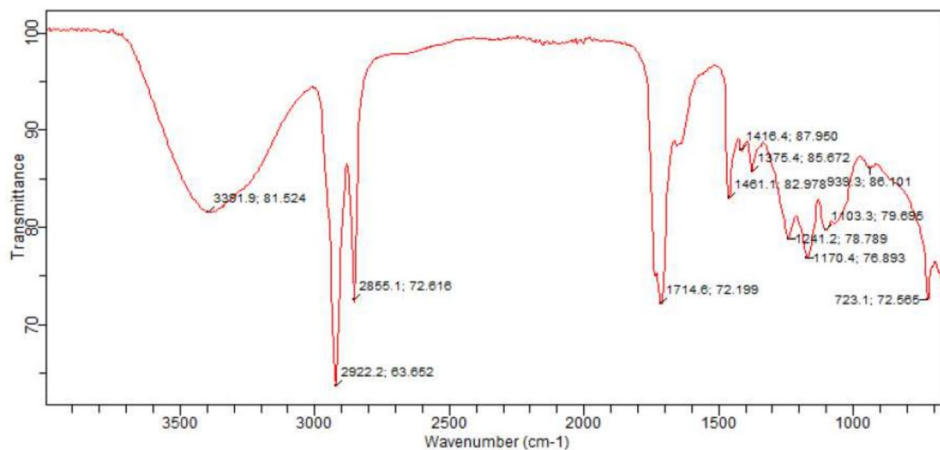


Fig. 7 GCMS graph for pure *Azadirachta indica* oil

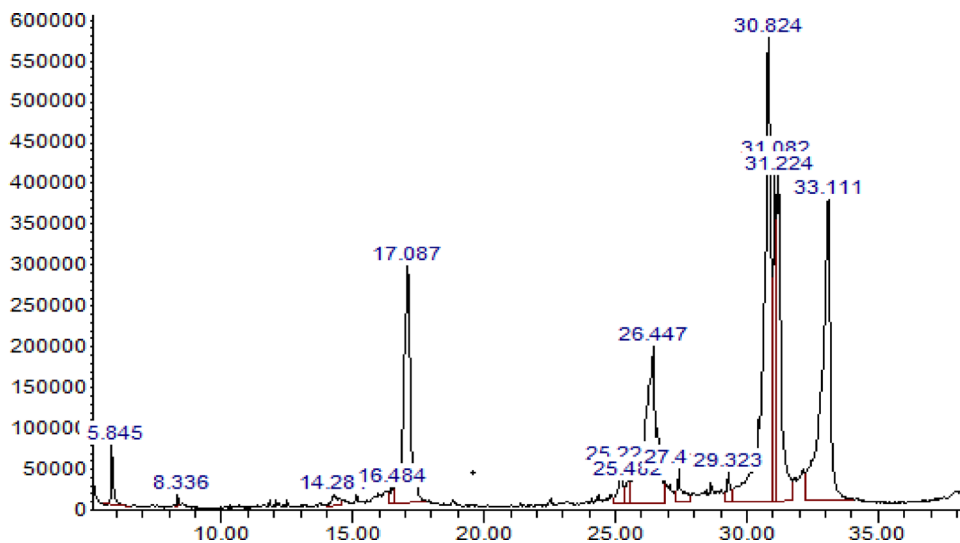


Table 9 Pure AISOs’ GCMS analysis

Retention time	Name of fatty acid	%wt
5.845	Palmitic acid	17.05
8.336	Oleic acid	5.312
14.28	Linoleic acid	56.32
16.484	Capric acid	2.19
17.087	Myristic acid	4.03
26.447	Arachidic acid	3.02
29.323	Ethylene brassylate	5.82
30.824	Fumaric acid	5.20
31.082	Pentanone	0.002
31.224	Stigmasterol	0.00015
33.111	Sitosterol	1.35

Table 10 Epoxidized AISOs’ GCMS analysis

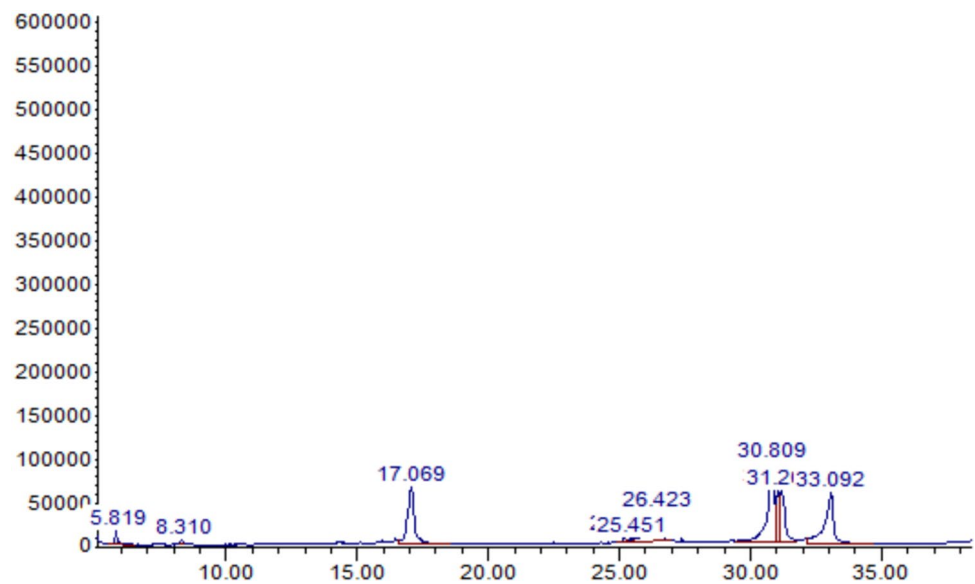
Retention time	Name of fatty acid	%wt
5.819	Palmitic acid	3.10
8.310	Stearic acid	5.10
17.069	Linoleic acid	48.32
25.451	Oleic acid	23.19
26.423	Pentanone	3.52
30.809	Stigmasterol	7.13
33.092	Sitosterol	10.56

Gas Chromatography–Mass Spectrometer (GC–MS)

The GCMS analysis in Table 9 presents AISOs’ constituents at various percentages. It showed eight peaks with their corresponding fatty acid values. Oleic acid (5.312%) and linoleic acid (56.32%) showed that *Azadirachta indica* oil contains fatty acid triglyceride, indicating its suitability

findings of Yigezu (2021) for *podocarpus falcatus* oil, Oke et al. (2021) for *Hevea Brasiliensis* oil, and Rizwan and Naseem (2018) for *Citrullus lanatus* oil (Fig. 7).

Fig. 8 GCMS for H₂SO₄ epoxy *Azadirachta indica* oil



for epoxide formation; Table 10 showed the development of the epoxides from AISO confirmed by the presence of pentanone (Serinyel et al. 2010); an epoxide formed during the decarboxylation process of the peroxyacetic acid on the oil. Stigmasterol and sitosterol, which are plant seed oil metabolites with a cholesterol structure, are enhanced during epoxidation and utilized in cosmetics and pharmaceutical industries (Cao et al. 1995; Ramadan 2015; Hang and Dusault 2010). The graphs in Figs. 7 and 8 identify the various peaks where the fatty acids and epoxides are formed. This result coincides with the findings of researchers who worked on the epoxidation of neem seed oil using a microwave-assisted melon seed peel catalyst by Nwosu-obieogu et al. (2022a).

Conclusion

This study successfully explored the potential of developing epoxides from AISO via process parameter impacts, modeling, optimization, and characterization using FTIR and GCMS. BBD was employed in the RSM analysis to model the relationship between the variables and the response. The 3D, contour, and ANOVA results confirm the model's acceptability and the process parameters significantly affect the response. The maximum oxirane value was actualized at a catalyst concentration (1.8), time (14,400 s), and temperature (50 °C). The normal probability plots depicted high predictability with the distributions of the points within the straight line. The experimental value of oxirane (5.134%) obtained at 1.2 concentration of catalyst, 14,400 s, and 50°C agreed with the predicted (RSM) value of 4.910% and PSO (5.172%) with minimum residual error. These significant

findings enable estimating and evaluating epoxides from AISO in the chemical industry and confirm the optimizations' techniques (RSM and PSO) rapid optimization of AISO epoxidation at a reduced time.

Funding None.

Availability of Data and Material None.

Code Availability None.

Declarations

Conflict of interest On behalf of all authors, the corresponding author states that there is no conflict of interest.

References

- Adepoju TF, Olawale O (2015) Optimization and predictive capability of RSM using controllable variables in *Azadirachta indica* oilseeds extraction process. *Int J Chem Mater Res* 3(1):1–10
- Aguele FO, Nwosu-Obieogu K, Osoh OK, Onyekwulu CS, Chiemenem LI (2021) Optimization of the epoxidation process parameters of huracrepitan seed oil. *Ann Fac Eng Hunedoara-Int J Eng* 1:61–68
- Anyu AU, Jack IR, Osagie OF (2016) Synthesis and characterization of oil-modified alkyd resin from epoxidized *Azadirachta indica* oil. *Am Chem Sci J* 15(2):1–7
- Association of Official Analytical Chemists (AOAC) (2003) Official methods of analysis of the Association of Official Analytical Chemists. Washington, DC, USA, p 17
- Cao J, Fales HM, Schaffner CP (1995) Cellular sterol accumulation stimulated by cholesterol 5 β , 6 β -epoxide in J774 macrophages. *Proc Soc Exp Biol Med* 209(2):195–204
- Dinda S, Ravisankar D, Puri P (2016) Development of bio-epoxide from Nahor (*Mesua ferrea* Linn.) oil. *J Taiwan Inst Chem Eng* 65:399–404

- Fang H, Zhou J, Wang Z, Qiu Z, Sun Y, Lin Y, Pan M (2022) Hybrid method integrating machine learning and particle swarm optimization for smart chemical process operations. *Front Chem Sci Eng* 16(2):274–287
- Goud VV, Patwardhan AV, Pradhan NC (2006) Studies on the epoxidation of mahua oil (*Madhunica indica*) by hydrogen peroxide. *Bioresour Technol* 97:1364–1371
- Hang J, Dussault P (2010) A concise synthesis of β -sitosterol and other phytosterols. *Steroids* 75(12):879–883
- Huang K, Lv F, Wu D, Wang Z (2019) Optimization of process conditions for styrene epoxidation based on the artificial intelligence method. *Chem Eng Technol* 42(6):1214–1222
- Jalil MJ, Habr HH, Abdul H, Mohd Yamin AF, Ismail KN, Abdul Rani NH (2020) Formation of dihydroxystearic acid (DHSA) from epoxidized palm oleic acid by peracid mechanism and their kinetic study. *J Mech Eng (JMEchE)* 17(3):85–94
- Jalil MJ, Azmi IS, Hadi A, Yamin AFM (2022) In situ hydrolysis of epoxidized oleic acid by catalytic epoxidation-peracids mechanism. *J Polym Res* 29(3):1–12
- Kadi MA, Akkouche N, Awad S, Loubar K, Tazerout M (2019) Kinetic study of transesterification using particle swarm optimization method. *Heliyon* 5(8)
- Kareemullah M, Afzal A, Rehman KF, KC V, Khan H, Soudagar ME, Kaladgi AR (2021) Preparation and physicochemical properties evaluation of epoxidized neem oil-based bio-lubricant. *Aust J Mech Eng* 21(3):942–951
- Khajeh M, Kaykhaei M, Sharafi A (2013) Application of PSO-artificial neural network and response surface methodology for removal of methylene blue using silver nanoparticles from water samples. *J Ind Eng Chem* 19(5):1624–1630
- Khayati GR (2020) A predictive model on the size of silver nanoparticles prepared by green synthesis method using hybrid artificial neural network-particle swarm optimization algorithm. *Measurement* 151:107199
- Matusiak M, Milchert E (2018) Optimization of selective epoxidation of Canola oil with in situ generated peracetic acid. *J Adv Oxid Technol* 21:1
- Milchert E, Smagowicz A, Lewandowski G (2010) Optimization of the reaction parameters of epoxidation of rapeseed oil with peracetic acid. *J Chem Technol Biotechnol* 85:1099–1107
- Nassef AM, Sayed ET, Rezk H, Abdelkareem MA, Rodriguez C, Olabi AG (2019) Fuzzy-modeling with particle swarm optimization for enhancing the production of biodiesel from microalga. *Energy Sources Part A Recov Util Environ Effects* 41(17):2094–2103
- Nwosu OK, Aguele F, Chiemenem L (2021) Synthesis of acrylated epoxidized biobased resin from groundnut seed oil. *Poljoprivredna Tehnika* 46(4):49–57
- Nwosu-Obieogu K, Umunna M (2021) Rubber seed oil epoxidation: experimental study and soft computational prediction. *Ann Fac Eng Hunedoara-Int J Eng pp.* 4
- Nwosu-Obieogu K, Aguele FO, Chiemenem LI (2020) Optimization on rubber seed oil epoxidation process parameters using response surface methodology. *Iran J Chem Chem Eng (IJCCCE)*. <https://doi.org/10.30492/ijcce.2020.40345>
- Nwosu-Obieogu K, Dzarma GW, Ugwuodo C, Chiemenem L (2022a) Environmental sustenance via melon seed peel conversion to fermentable sugars using soft computing models. *Clean Eng Technol* 7:100452
- Nwosu-Obieogu K, Dzarma GW, Ugwuodo CB, Chiemenem LI, Akatobi KN (2022b) Luffa seed oil extraction: response surface and neuro-fuzzy modelling performance evaluation and optimization. *Process Integr Optim Sustain* 6(1):175–188
- Nwosu-Obieogu K, Adeyi O, Dzarma G (2022c) Response surface methodology and artificial neural network modeling and optimization of *Colocynthis vulgaris* shrad peel sulphuric acid hydrolysis. *Clean Circ Bioecon* 100019
- Nwosu-Obieogu K, Agu CM, Dzarma GW, Awele AM, Nkemakolam A (2022d) Microwave-assisted carbon-based sulfonated melon seed peel catalyst development for the optimization of AISO epoxidation using response surface methodology. *Clean Mater* 4:100069
- Nwosu-Obieogu K, Grace E, Dzarma GW, Aguele FO, Chiemenem LI, Gabriel O, Maureen AA, Ekeoma N (2024) Melon seed oil epoxidation: kinetics and neuro-fuzzy evaluation. *S Afr J Chem Eng* 47(1):169–177
- Oke EO, Adeyi O, Okolo BI, Adeyi JA, Ayanyemi J, Osoh KA, Adegoke TS (2020) Phenolic compound extraction from Nigerian *Azadirachta indica* leaves: response surface and neuro-fuzzy modelling performance evaluation with Cuckoo search multi-objective optimization. *Results in Engineering* 8:100160
- Oke EM, Nwosu-Obieogu K, Okolo BI, Adeyi O, Ude UC (2021) *Hevea brasiliensis* oil epoxidation: hybrid genetic algorithm-neural fuzzy-Box Bhenken (GA-ANFIS-BB) modeling with sensitivity and uncertainty analyses. *Multiscale Multidiscipl Model Exp Design* 1:1–15
- Okieimen FE, Bakare OI, Okieimen CO (2002) Studies on the epoxidation of rubber seed oil. *Ind Crops Prod* 15:139–144
- Onoji S, Iyuke S, Igbafe IA, Daramola OM (2017) *Hevea brasiliensis* (rubber seed) oil: modeling and optimization of extraction process parameters using response surface methodology and artificial neural network techniques. *Biofuels* 6:1–15
- Poyraz Ç, Küçükıldız G, Kırbaşlar Şİ, Ciğeroğlu Z, Şahin S (2021) Valorization of *Citrus unshiu* biowastes to value-added products: an optimization of ultrasound-assisted extraction method using response surface methodology and particle swarm optimization. *Biomass Convers Biorefin* 1–11
- Ramadan MF (2015) Oxidation of β -sitosterol and campesterol in sunflower oil upon deep-and pan-frying of French fries. *J Food Sci Technol* 52(10):6301–6311
- Rao MS, Venkaiah N (2015) Parametric optimization in machining of Nimonic-263 alloy using RSM and particle swarm optimization. *Procedia Mater Sci* 10:70–79
- Rizwan M, Naseem S (2018) Characterization of epoxidized high contents of linoleic and oleic fatty acids of *Citrullus lanatus* seed oil. *Am J Chem Appl* 5(1):1–9
- Saad MS, Mohd Nor A, Zakaria MZ, Baharudin ME, Yusoff WS (2021) Modeling and evolutionary computation optimization on FDM process for flexural strength using integrated approach RSM and PSO. *Progr Addit Manuf* 6(1):143–154
- Sahu H, Mohanty K (2017) One pot peroxidation of oleic acid-rich *Azadirachta indica* oil over bio-waste derived heterogeneous catalyst. *Can J Chem Eng* 95(8):1526–1536
- Sarkar T, Salaududdin M, Hazra SK, Chakraborty R (2020) Comparative study of predictability of response surface methodology (RSM) and artificial neural network-particle swarm optimization (ANN-PSO) for the total color difference of pineapple fortified rasgulla processing. *Int J Intell Netw* 1:17–31
- Serinyel Z, Chaumeix N, Black G, Simmie JM, Curran HJ (2010) Experimental and chemical kinetic modeling study of 3-pentanone oxidation. *J Phys Chem A* 114(46):12176–12186
- Turco R, Tesser R, Russo V, Vitiello R, Fagnano M, Di Serio M (2019) Comparison of different possible technologies for epoxidation of *Cynara cardunculus* seed oil. *Eur J Lipid Sci Technol* 1900100:1–8
- Yash Roy RC, Gupta PK (2000) *Azadirachta indica*-seed oil inhibits growth of termite surface tunnel. *Indian J Toxicol* 7:49–50

Yigezu M (2021) Epoxidation of *Podocarpus falcatus* oil by sulphuric acid catalyst: process optimization and physicochemical characterization. Am J Chem Eng 9(4):84–90

Publisher's Note Springer Nature remains neutral with regard to jurisdictional claims in published maps and institutional affiliations.

Springer Nature or its licensor (e.g. a society or other partner) holds exclusive rights to this article under a publishing agreement with the author(s) or other rightsholder(s); author self-archiving of the accepted manuscript version of this article is solely governed by the terms of such publishing agreement and applicable law.